Lecture 19
Surface vibrations

Variety: IR, Raman, EELS, inelastic neutron tunneling, helium atom scattering, STS

Most spectroscopies see, v = 0 to v= 1

$E_v = (v+1/2)\ hv$

v is the quantum number

$v = 1/2\pi\sqrt{(k/\mu)}$

$\mu = m_1m_2/m_1+m_2$

High resolution electron energy loss spectroscopy HREELS

Other methods to study surface vibrations

1. Inelastic electron tunneling

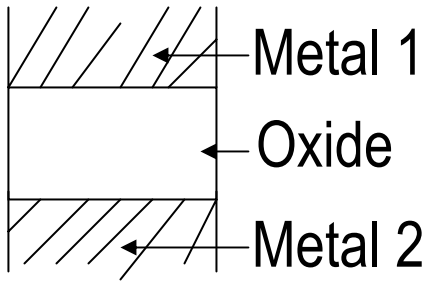

For $eV_0 > \hbar \omega_0$

When voltage is varied, a new tunneling channel opens up.

The junction conductance $G(V_0) = dI/dV_0$ jumps discontinuously.

An important problem is thermal smearing of the Fermi Surface of the solid. This limits studies only at low temperatures.

2. Raman scattering
3. IR reflectivity of metal surfaces
4. Low energy atom beam scattering

Basic instrument

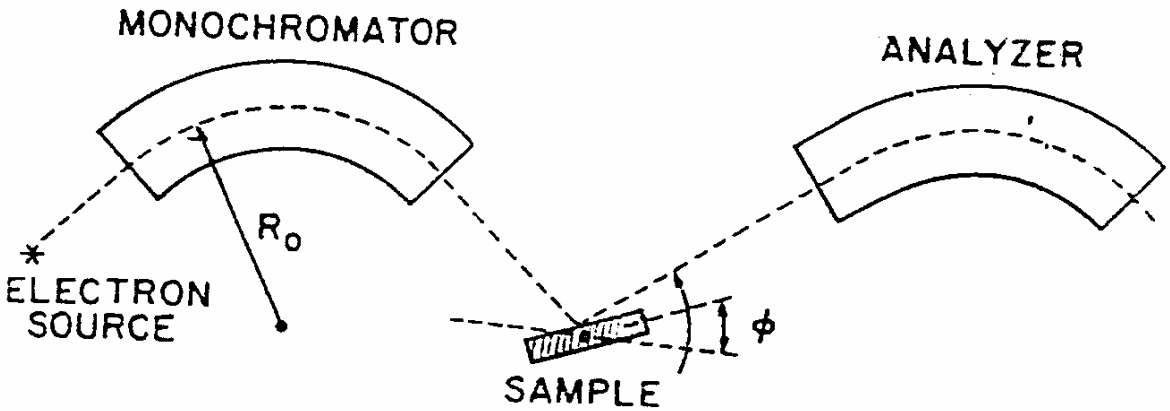

Fig. 1.1 Schematic diagram of an electron energy loss experiment. Electrons from a cathode pass through a monochromator, strike the sample, and the energy spectrum of the scattered electrons is probed by a second monochromator.

The technique is only for solid surfaces.

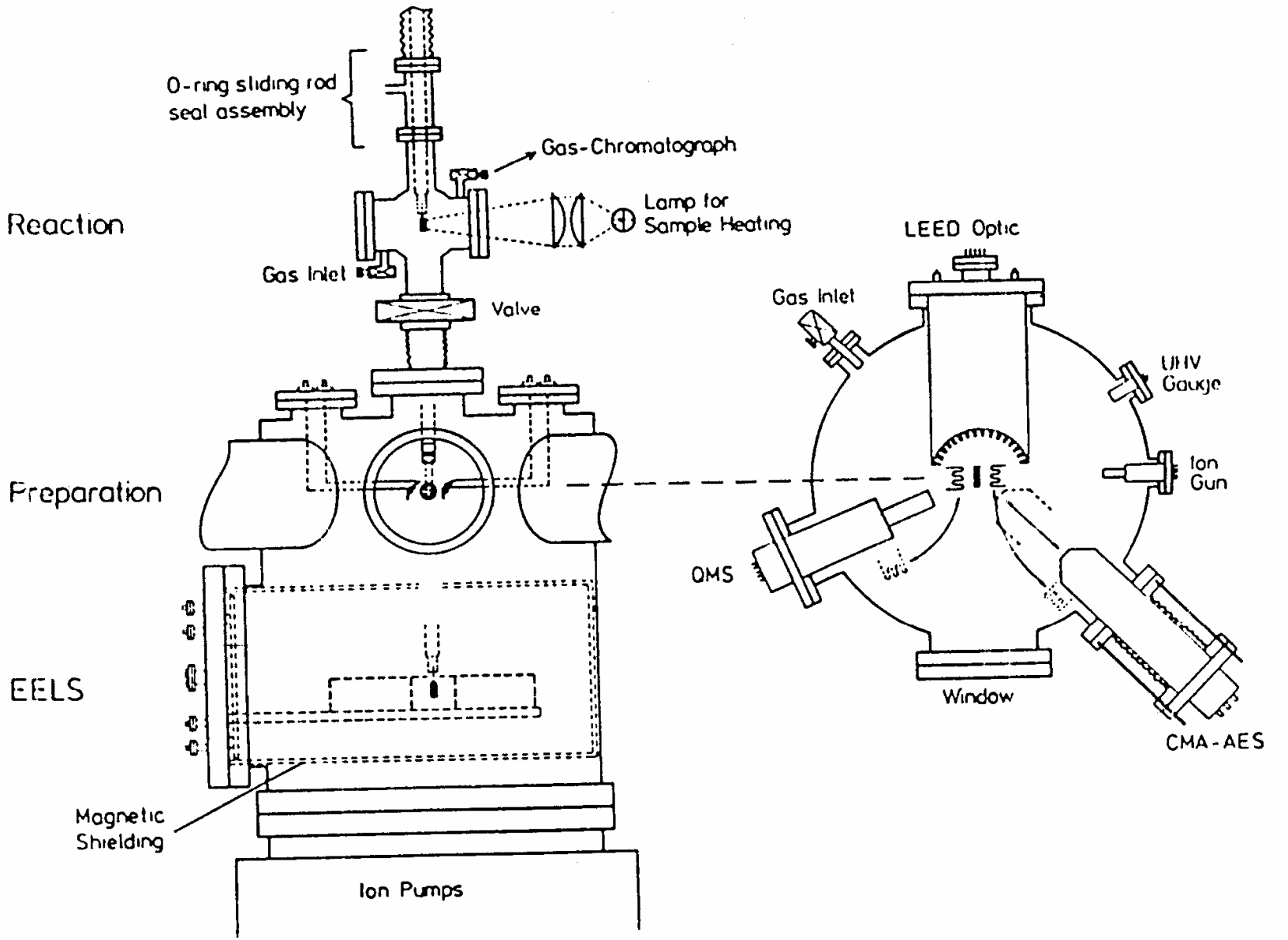

The spectrometer has many other facilities, normally.

One needs high intensity to do a measurement
It is always an adjustment..

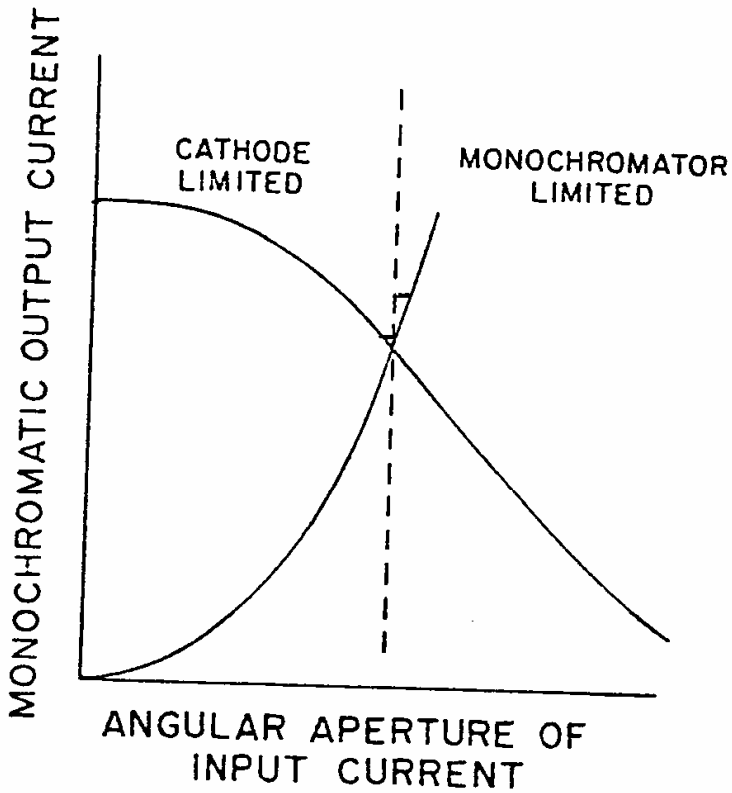

Fig. 2.2 Qualitative sketch of the output current of a monochromator fed by a cathode system as a function of the angular aperture. The monochromatic current is either limited by the input current as supplied by the cathode (cathode limited) or by the maximum current that can be properly handled by the monochromator.

It helps to study adsorbate orientation

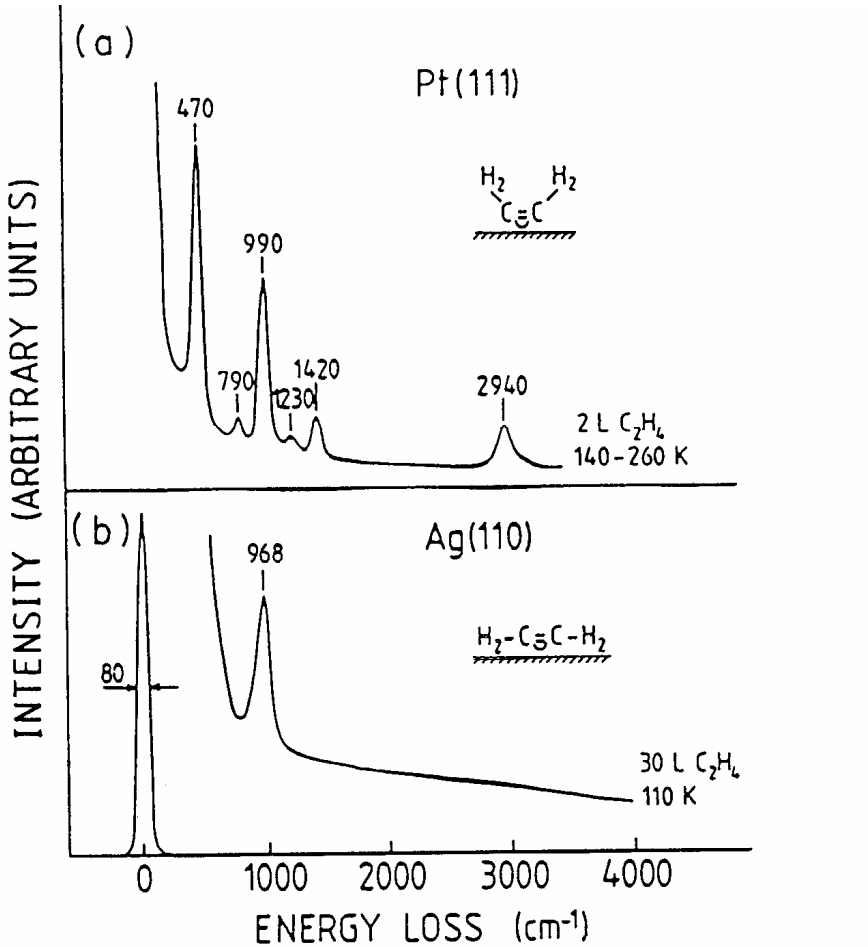

Fig. 4.9 Electron energy loss spectrum in specular reflection for ethylene on (a) Pt(111) and (b) Ag(110) (from Ibach and Lehwald [28], and Backx, de Groot, and Biloen [13], used with permission). For ethylene on silver, the surface hardly breaks the symmetry of the molecule. Therefore only the B_{1u} CH wagging mode with its dipole moment perpendicular to the plane of the molecule becomes observable as a dipole loss. The orientation of the molecule follows automatically from these considerations since the strongly IR-active B_{2u} and B_{3u} modes (see also frequency tables, Appendix B) which have their dipole moment oriented within the plane of the molecule, are not observed for the adsorbed molecule. On the platinum surface ethylene is strongly bonded. This is indicated by the CH stretching vibration which is typical for an sp^3 complex. Strong bonding to the surface breaks the symmetry and new modes become dipole active.

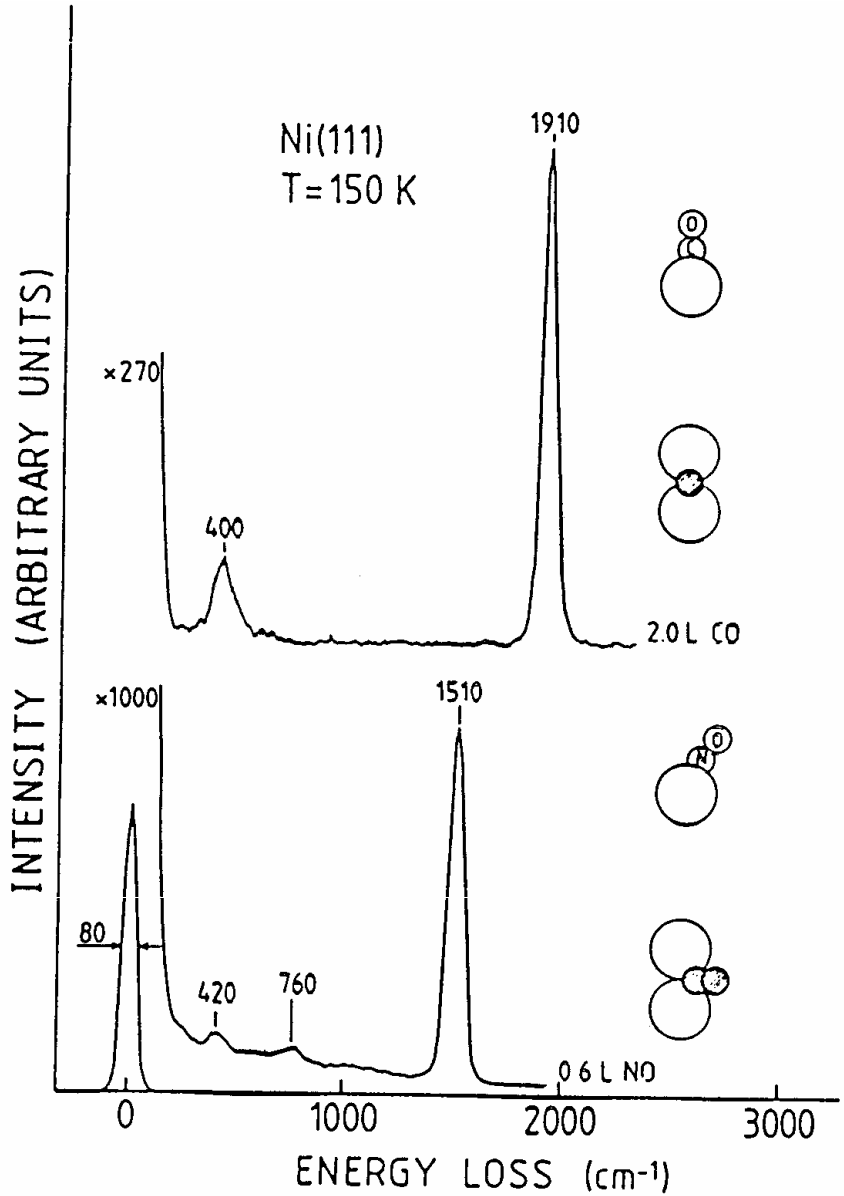

Fig. 4.11 Spectra of CO and NO on a Ni(111) surface at $T = 150$ K (from Erley, Wagner, and Ibach [15], and Lehwald, Yates, and Ibach [16], used with permission). The two losses for CO correspond to the CO stretching and the Ni–C stretching vibration. The canted orientation of NO makes the Ni–N–O bending mode dipole active as well.

TABLE 6.1

Vibrational Frequencies of Atoms Perpendicular to the Surface for Different Ligancies and (Fundamental) Frequencies of Equivalent Diatomic Molecules[a]

System	Ligancy 4	Ligancy 3	Ligancy 2	Diatomic molecule	Ref.	Comment
O–W	610		740	1047	5	
O–Ni	430/310	580/450		~615	6–8	Two binding states
O–Pt		490		841	9	
O–Fe		400	500	~870	10	Fe atoms not in contact
O–Ru		515		865	11	
O–Cu	340				12	
H–Ni	600 (590)	(1210)	(1370)	~1926	13, 19	Values in parentheses are calculated [19]
H–Pt		550		~2200	14	Only ω_e known for PtH
C–Ni	390	520			15	
S–Ni	360				16	

[a] Cf. Appendix B. For oxygen on nickel, two different binding states are observed.

Adsorption of CO

Frequencies allow us to understand the kind of adsorption

2130 – 2000 cm^{-1}	Terminal CO	m – CO
2000 – 1880 cm^{-1}		m_2 - CO
1880 – 1800 cm^{-1}		m_3 – CO
< 1800 cm^{-1}		m_4 – CO

TABLE 6.3

CO Stretching and Metal Carbon Frequencies of Adsorbed CO on Various Crystal Surfaces[a]

Substrate	ν_{M-C}	ν_{CO}	Site	Ref.
Fe(110)	455	1890	Top	31
Ni(100)	480	2065	Top	32
	360	1930	Bridge	
Ni(111)	400	1810	Threefold bridge	33
Cu(100)	340	2090	Top	34
Ru(001)	445	1990	Top	35
Rh(111)	480	1990	Top	36
Pt(111)	480	2105	Top	37
	380	1870	Bridge	101
W(100)	365	2080	Top	38

[a] Data refer to low coverage except for the last two entries

Orbital picture

5σ and 2π are the orbitals involved

There are two effects

$M \rightarrow 2\pi^*$ |

$M \leftarrow 5\sigma$ | charge – transfer

Higher ligancy increases the π overlap and force constant decreases

Vibrational frequencies (dipole active) of oxygen or Ni, Pt, and Fe for various states of oxidation.

	Adsorbed	Intermediate	Bulk oxide
Ni(111)	580	950[b]	545[c]
Ni(100)	435	910[c]	545[c]
Pt(100)	490	720[d]	
Fe(110)	500[e]	910[e]	660 Fe_2O_3[f]

[a] For Ni see also Table 6.1.
[b] 950 cm^{-1} is enhanced when oxygen is brought on to the surface by decomposing NO [24].
[c] Ref. [25].
[d] Produced by high-temperature treatment in O_2 [26].
[e] Produced by high-temperature treatment in O_2 [10].
[f] Highest LO-phonon frequency of Fe_2O_3 [27].
Data for [a–f] are used with permission.

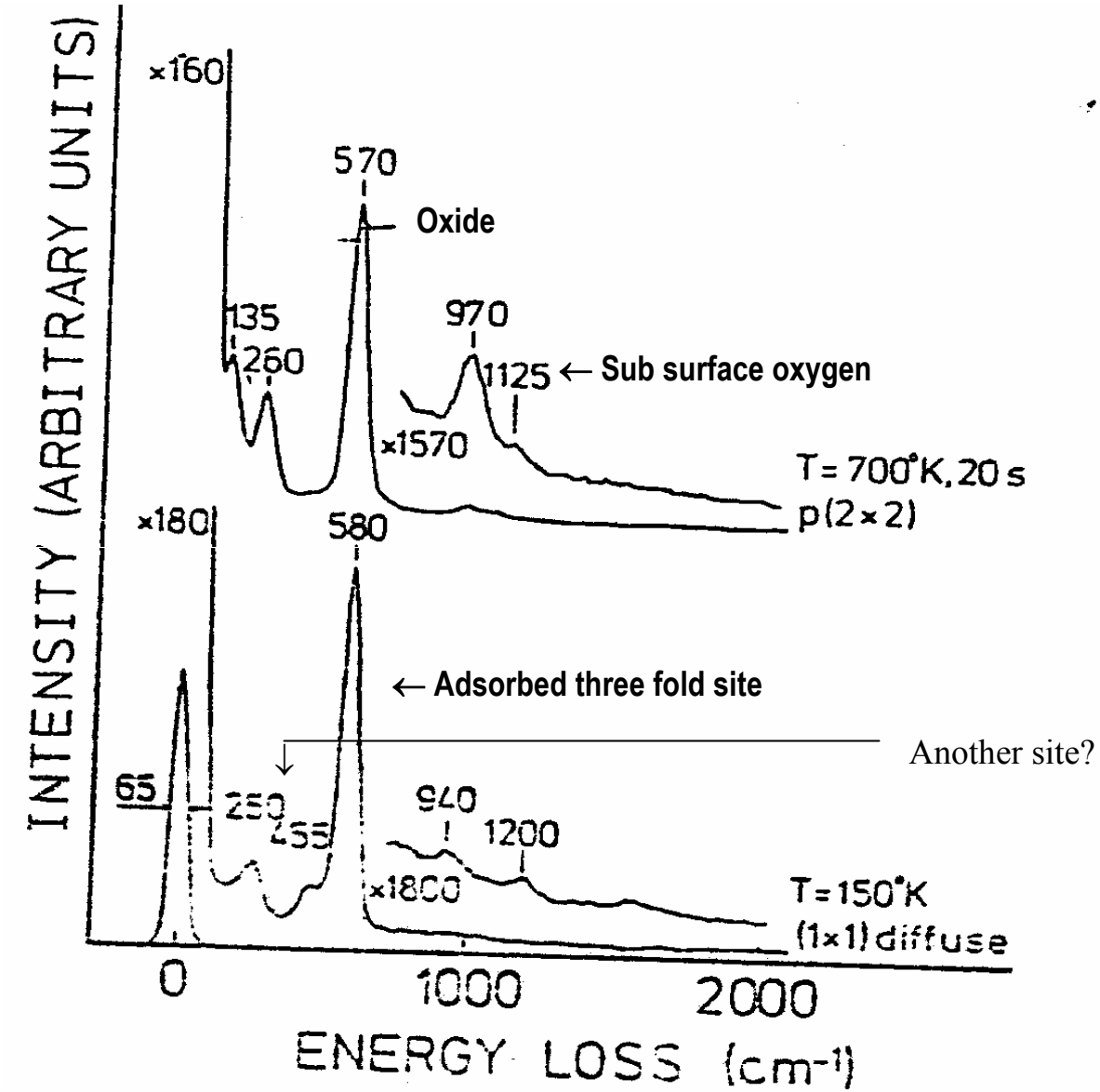

Oxygen on Ni(111) after exposure at 150 K 2L.

Decomposition of NO

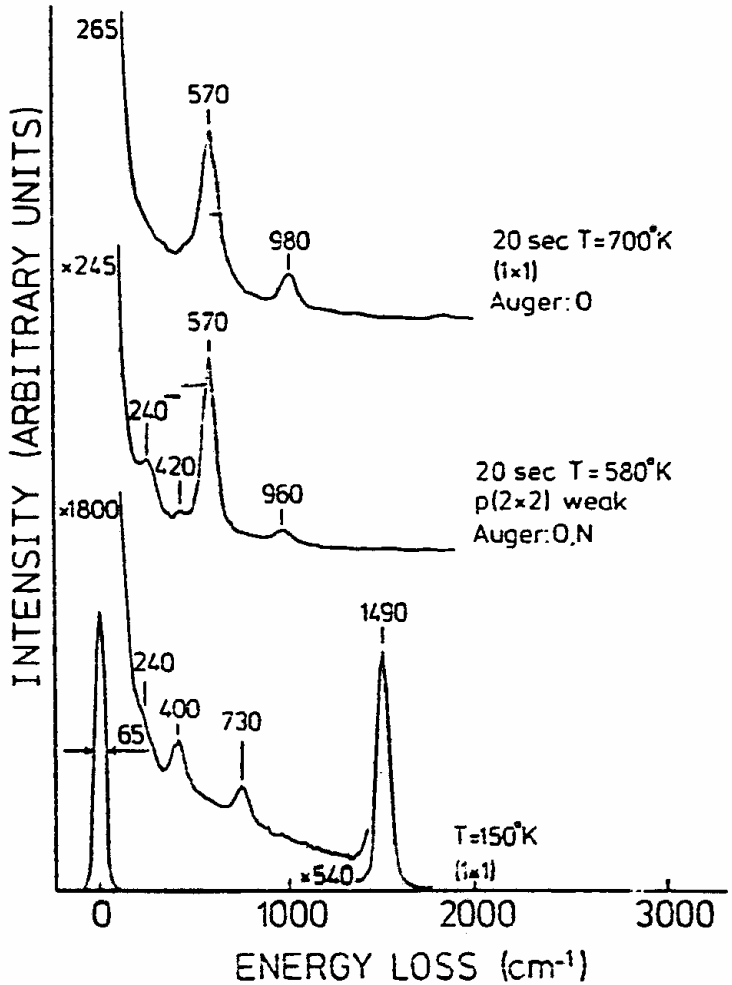

Fig. 6.5 Decomposition of NO by annealing the surface to 580 and 700°K at 0.5 langmuir After annealing to 700°K the surface is nitrogen free since nitrogen desorbs. Again the remaining oxygen spectrum exhibits a peak at about 980 cm^{-1}, this time with an even greater intensity than in Fig. 6.4.

CC Stretching frequencies, C-C bond order, and CH stretching vibration for acetylene and ethylene on nickel

Adsorption system	ν_{CC}	n	ν_{CH}
C_2H_2–Ni(111)	1200	~1.1	2920
C_2H_2–Pt(111)	1310	~1.3	3010
C_2H_4–Pt(111)	1230	~1.2	2940

TABLE 6.6

Innermolecular Bond Distance of Adsorbed CO and NiO Bond Distances as Determined by Electron Diffraction (d_{exp}) Compared to Distances Calculated from the Apparent Stretching Force Constant using Badger's Rule

Adsorption system	d_{exp} (Å)	d_{th} (Å)	f (10^5 dyn cm^{-1})
CO–Ni(100)	1.10 ± 0.1 [41]	1.14	17.2
CO–Cu(100)	1.15 ± 0.05 [41]	1.14	17.5
O–Ni(100)	1.97 ± 0.05 [70]	1.98 ± 0.03	1.65
O–Ni(111)	1.87 ± 0.05 [71]	1.91 ± 0.03	2.0

Overtones and bond energy

Birge-Sponer extrapolation

$D_0 = \omega^2/h\omega_e x_e - 1/2\ \omega_e + 1/4\ \omega_e x_e$

$\omega_e = 3\nu^1 - \nu^2$

$\omega_e x_e = \nu^1 - 1/2\ \nu^2$

ν^1 = fundamental, ν^2 = overtone

TABLE 6.7

Fundamental Frequencies and First Overtones for Several CH Groups and Molecular Oxygen on Silver[a]

Adsorption system	$\nu^{(1)}$	$\nu^{(2)}$	$\bar{D}_0$ (eV)	D (eV)
C_2H_2–Ni(111)	2920	5730	5.0 ± 0.5	4.27 [58]
1 L C_2H_4–Ni(100)	2920	5680	3.5 ± 0.5	
	3010	5860	3.7 ± 0.5	
3 L C_2H_4–Ni(100)	2780			
	2990	5850	4.5 ± 0.5	
O_2–Pt(111)	875	1645	0.5 ± 0.08	~0.35 [26]

[a] Bond energies D_0 are estimated with Eq. (6.12) and compared with the standard CH bond energy and the activation energy for dissociation of molecular oxygen on platinum [26], used with permission.

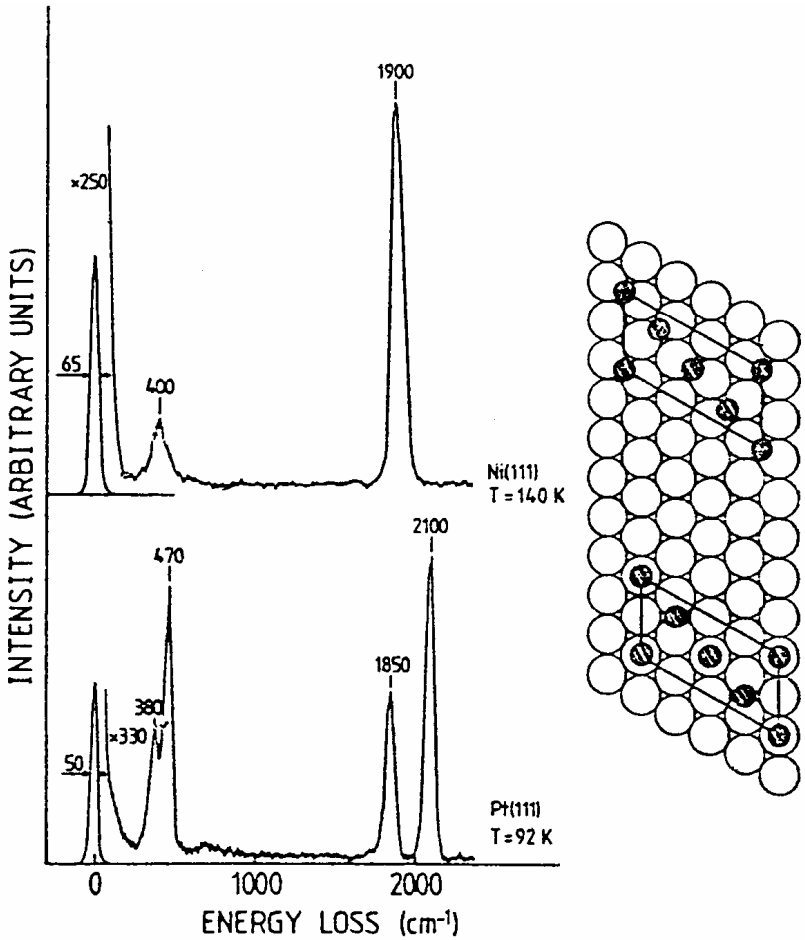

Fig. 6.7 Electron energy loss spectra of the Ni(111) and Pt(111) surfaces each covered with half a monolayer of CO which orders into a $c(4 \times 2)$ overlayer. On the nickel surface the vibration spectrum indicates only a single CO species in a site of high symmetry. The only possibility for positioning the two-dimensional CO lattice on the surface consistent with the single type of adsorption site is to place all CO molecules into twofold bridges. By similar reasoning, half the CO molecules must occupy on-top sites on the Pt(111) surface. This example shows how powerful the *in situ* comparison of vibrational spectra and diffraction pattern can be, since a qualitative structure analysis is achieved without analyzing diffraction intensities.

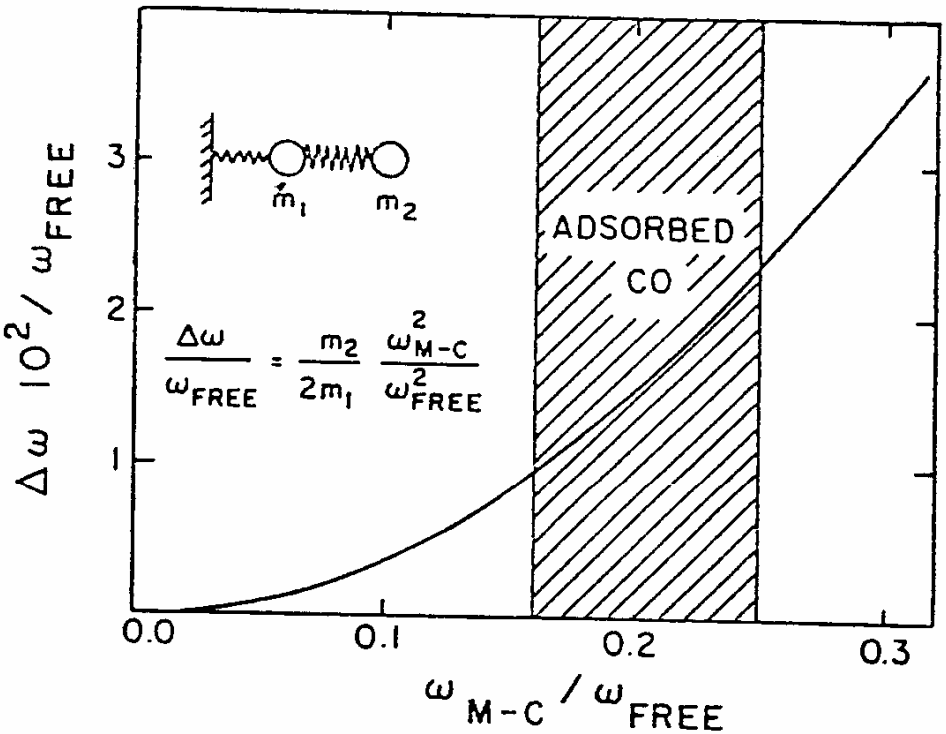

Fig. 6.14 Ratio of the shift of the stretching frequency of adsorbed CO to the frequency of the free molecule versus the ratio of the metal–carbon stretching frequency to the frequency of the free molecule calculated in the nearest-neighbor force constant model assuming the mass of the surface atom to be infinitely large. The shaded area represents the typical range for chemisorbed CO.

Origin of frequency shifts

1. Mechanical renormalisation $\sim 40 cm^{-1}$
2. Lateral interactions $\sim 30 cm^{-1}$
3. Bond order
   This is the most important effect. Eg. C ≡ C vibration of acetylene (at about 2000 cm^{-1}) get reduced to1200 cm^{-1} on Ni.
4. Hydrogen bonding

Empirical fits

Force constant and bond parameters

$f \sim 5. \times 10^{-4} De^2$

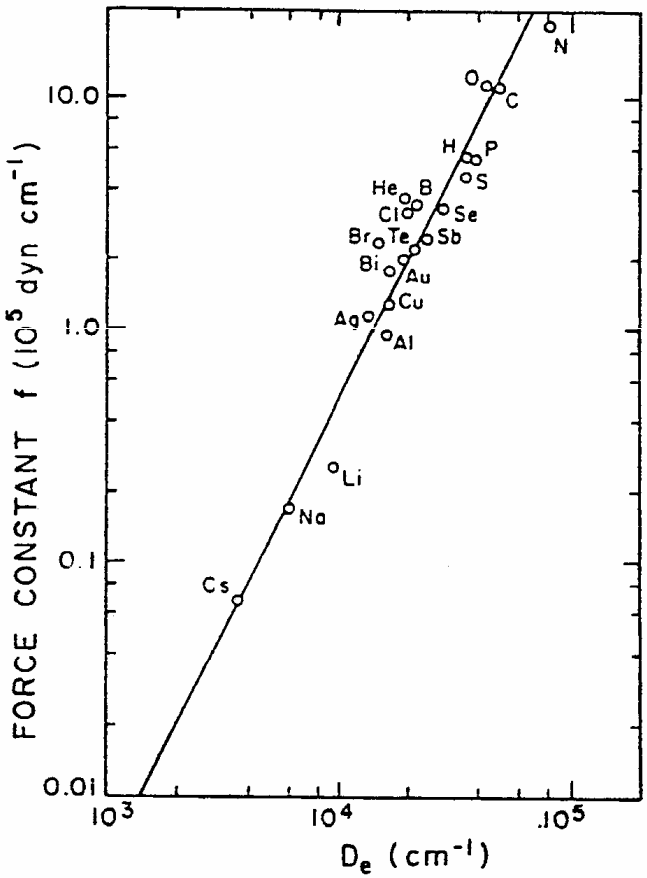

Fig. 6.15 Harmonic force constants versus depth of the potential well D_e for diatomic molecules (data from Ref. [B3] used with permission). Values for the C–C bond in hydrocarbons are also included.

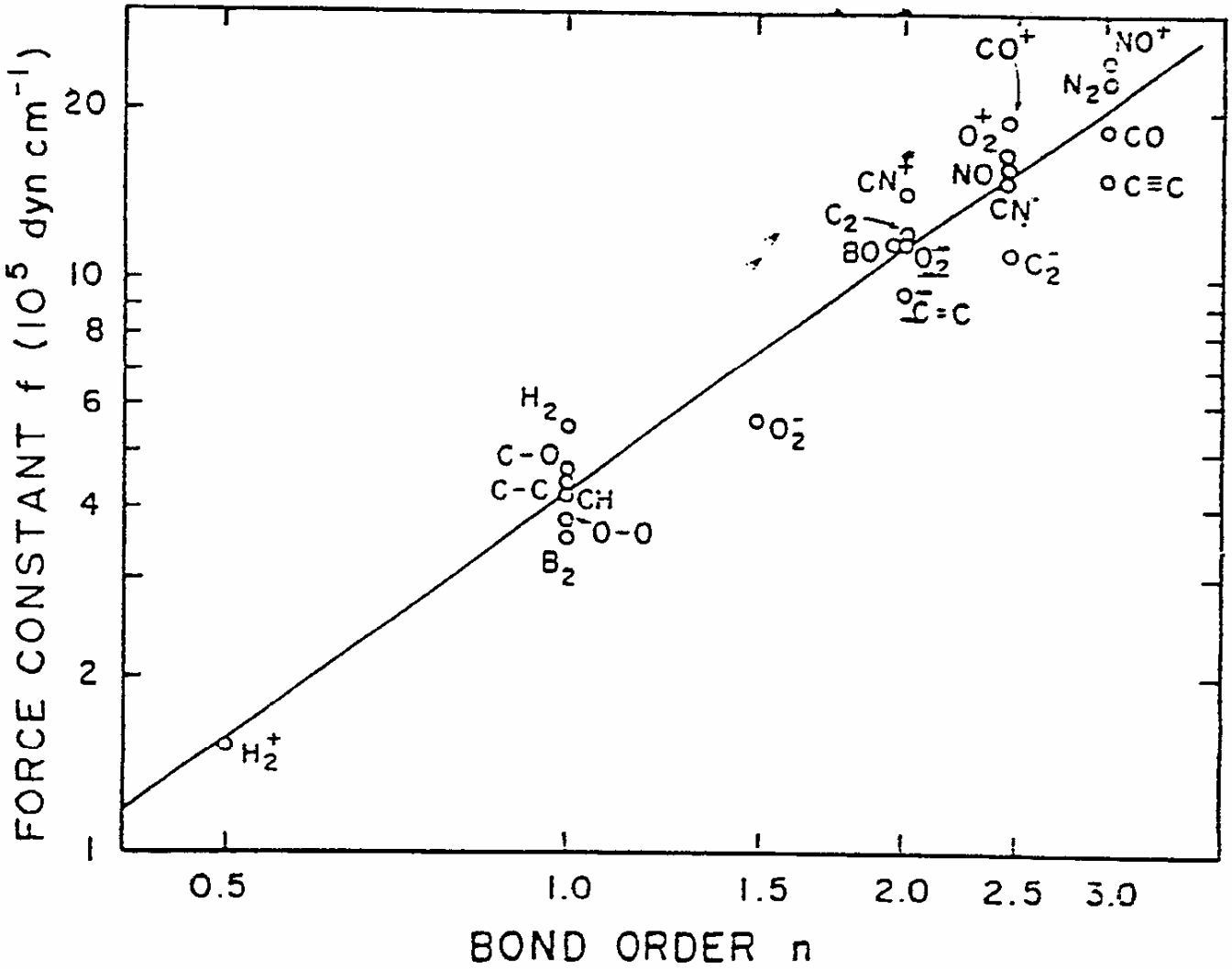

Fig. 6.17 Correlation between bond order as defined in the text and the force constant; again CC— bonds of hydrocarbons and the single bonds of ⩾C—O— and HO—OH are included.

$$f = 4.2 \times 10^5 \, n^{1.45} \text{ (dyne/cm)}$$

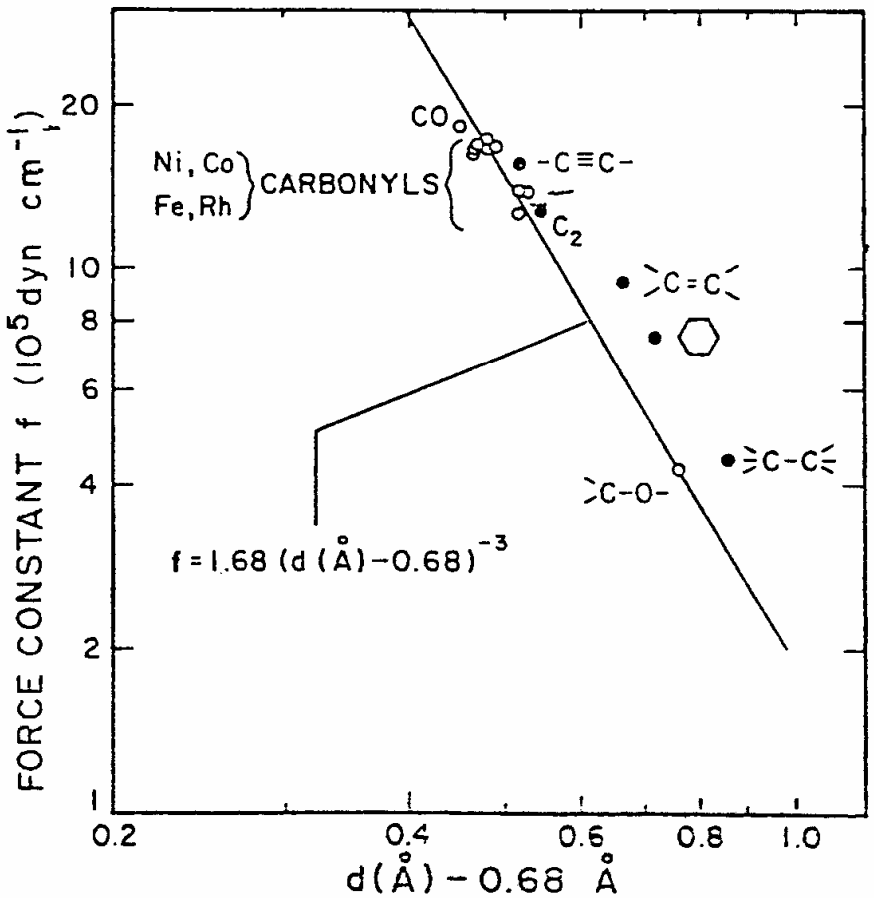

Fig. 6.18 Force constants of CO— and CC— groups versus bond distance. For the CC— groups data are from Ref. [57] with permission. The carbonyl data are from Ref. [62] with permission. There the force constants have been calculated disregarding the coupling to the metal ligand.

$$f = 1.86\,(r_e - d_{ij})^{-3} \qquad d_{ij} = 0.68\ \text{Å}$$

Hydrogen bonding

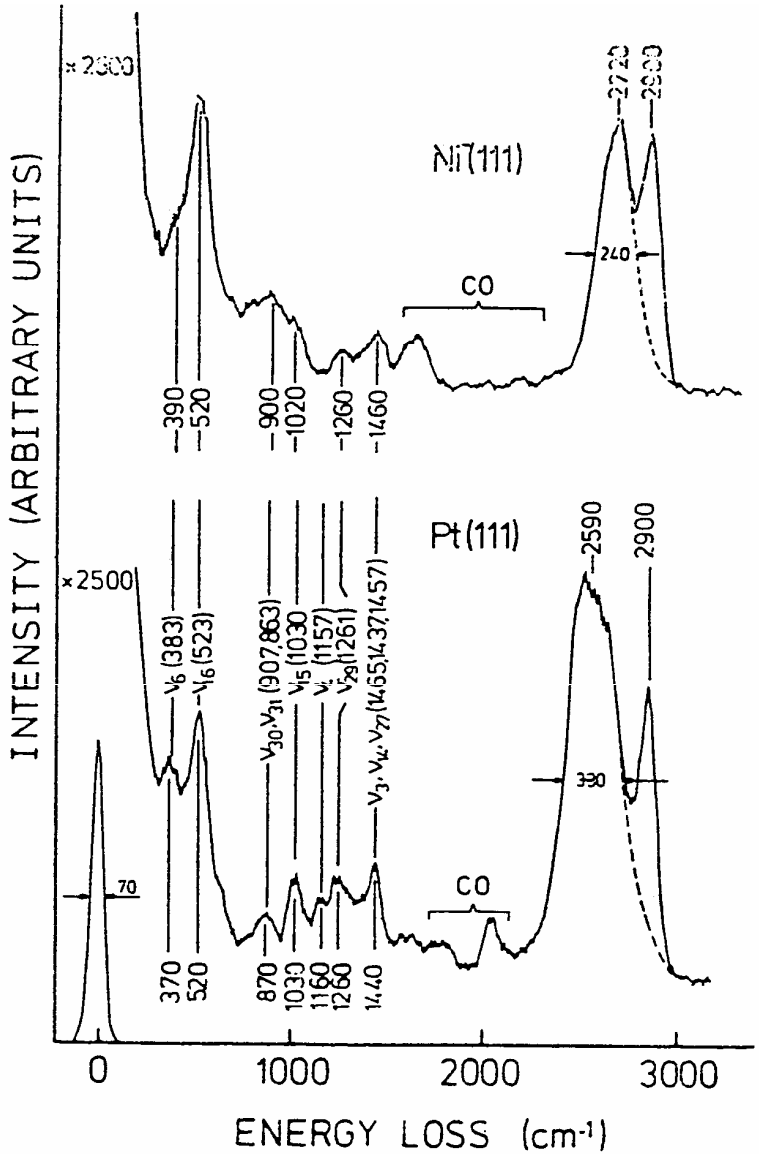

Fig. 6.19 Spectrum of cyclohexane (C_6H_{12}) adsorbed on Ni(111) and Pt(111) at $T = 140$ K ([71] used with permission). All vibrations can be assigned to the A_{1g}, A_{2u}, E_g, and E_u modes of C_6H_{12}. Using the dipole selection rule and the correlation tables (Table 4.6), this indicates a symmetry C_s. It is therefore likely that cyclohexane assumes a canted position with three hydrogens pointing towards the surface. The hydrogen atoms give rise to the strong broad CH stretching band suggesting hydrogen bonding on the molecule to the surface.

Dissociation reactions

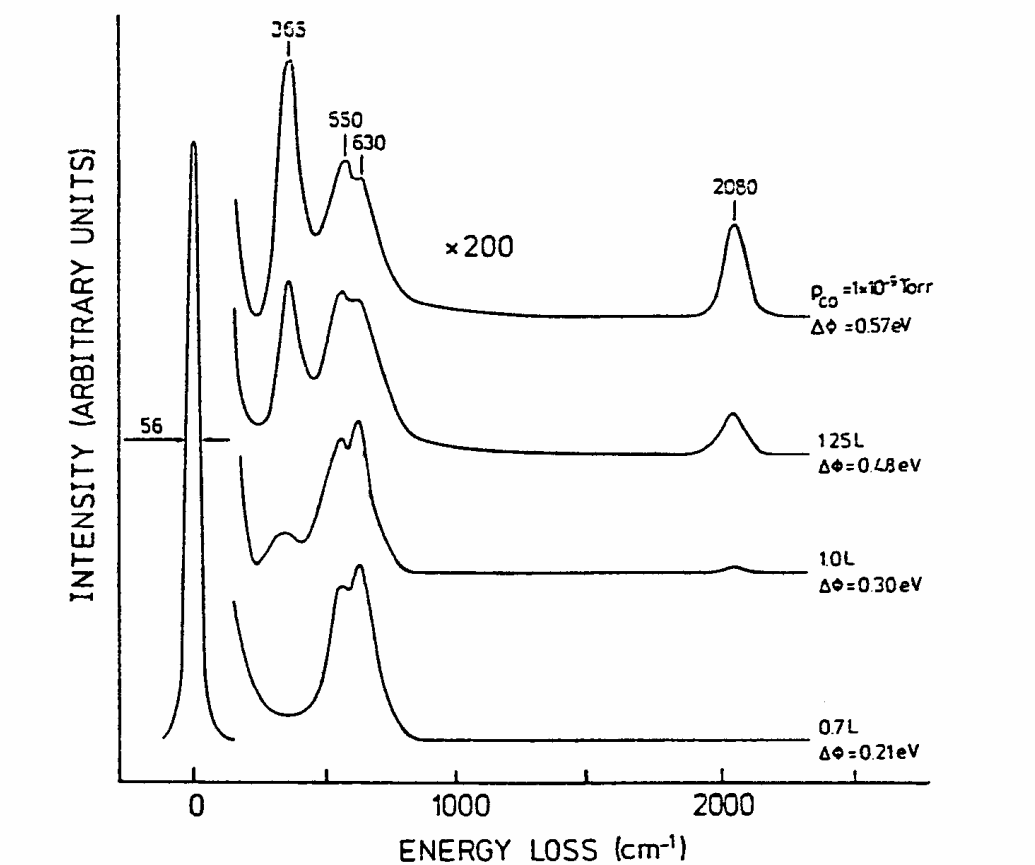

Fig. 6.23 Spectra of W(100) after CO exposure at ~300°K. At low coverage no molecular CO is observed. The two energy losses at 550 and 630 cm^{-1} are identified as due to vibrations of carbon and oxygen by decomposing C_2H_2 on the surface and exposure to oxygen, respectively [38] (used with permission). With higher exposure molecular CO is also adsorbed. Saturation coverage is not reached at room temperature without an ambient pressure of CO.

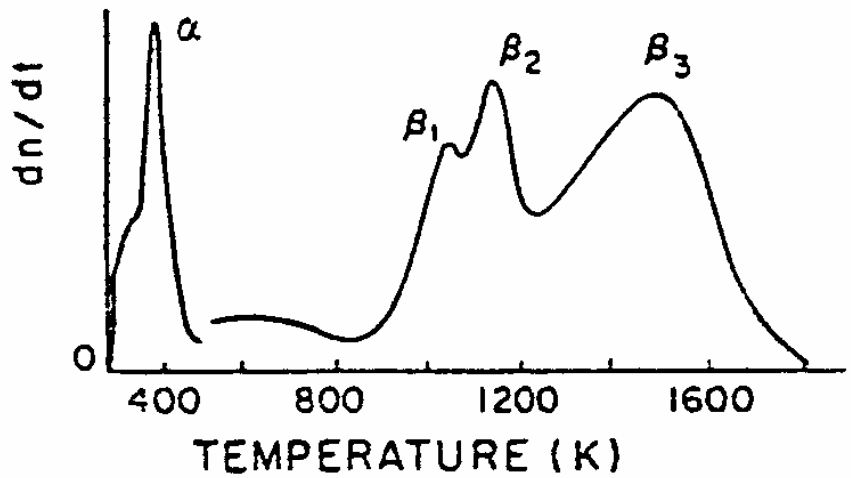

Fig. 6.24 Flash desorption trace of CO on W(100) after Clavenna and Schmidt ([85] used with permission). All peaks refer to molecular desorption of CO and the surface is clean after the CO desorption is completed. This has mislead researchers to assume that the "β states" refer to different forms of *molecular* CO on the surface. Vibration spectroscopy has shown however that only the α peak represents desorption of molecular CO which was in a *molecular state prior* to the desorption process. The different structures in the high temperature regime all result from recombinative desorption of oxygen and carbon. The structures reflect the kinetics of this process, not different types of binding states at room temperature.

A complex reaction at the surface

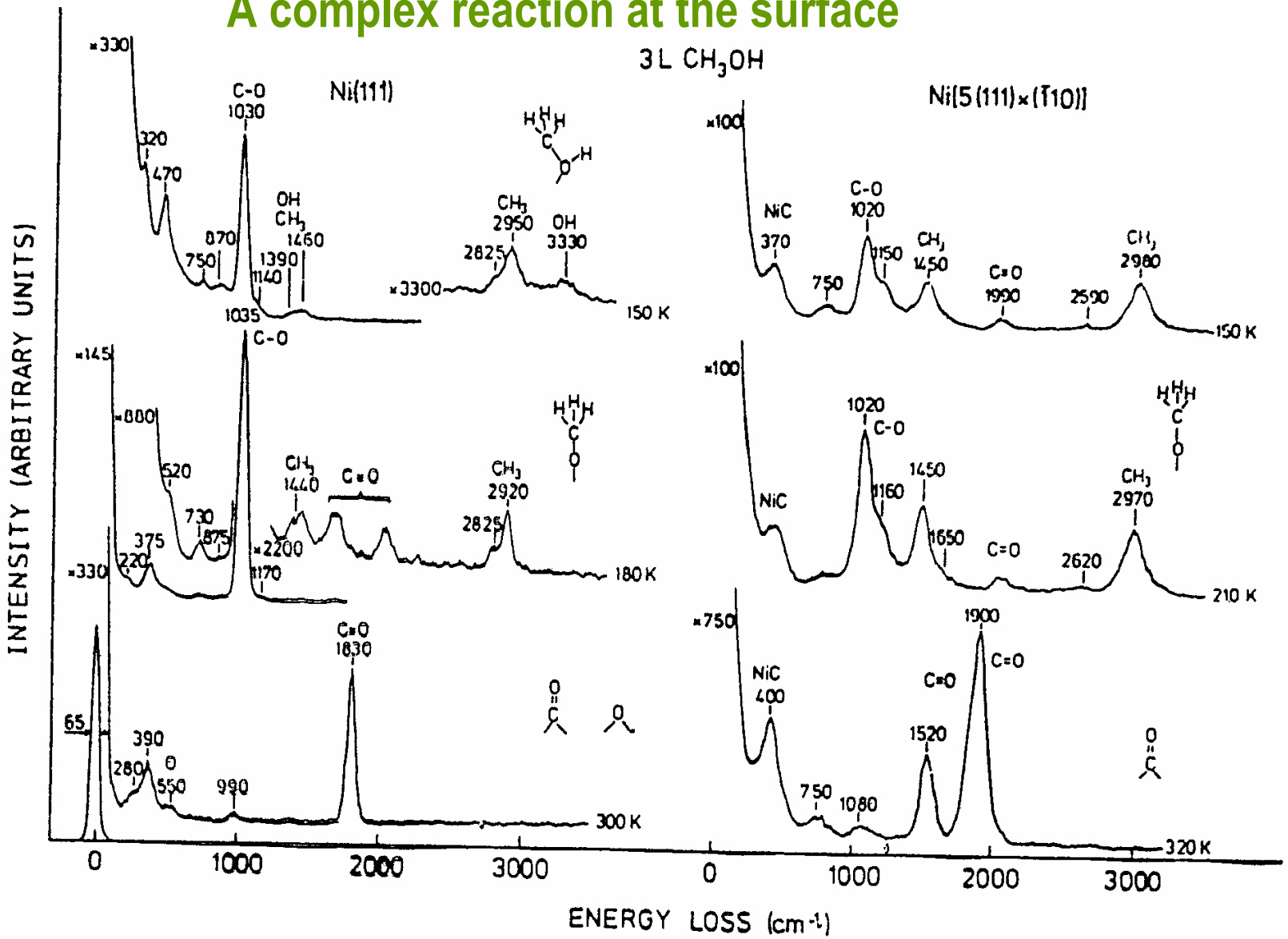

Fig. 6.27 The decomposition of methanol on Ni(111) and a stepped nickel surface with (111) terraces via an intermediate methoxy group. Earlier spectra of methanol on Ni(111) ([87], used with permission) were not completely free of water which is quite noticeable even when the fractional coverage is only 1%.

Surface species

Ni(111)

$$CH_3\,OH_{gas} \xrightarrow{150\ K} CH_3OH$$

$$CH_3OH \xrightarrow{180\ K} CH_3O + H$$

$$CH_3O \xrightarrow{300\ K} CO + H + C + O$$

$$2H \xrightarrow{380\ K} H_{2\,gas}$$

$$CO \xrightarrow{460\ K} CO_{gas}$$

$$C + O \xrightarrow{850\ K} CO_{gas}$$

Ni(5(111) x 110)

$$CH_3OH_{gas} \xrightarrow{<150\ K} CH_3O + H + CO$$

$$CH_3O \xrightarrow{320\ K} CO + H + \text{decomposition products}$$